The local force-displacement impact response of the cranium is dependent on cranial region and the presence of the scalp

Nienke S. Reitsma, Darcy Thompson-Bagshaw, Zoe Glover, Baptiste Sandoz, Claire F. Jones.

Abstract The mechanical response of the cranium to localised impact may be specific to bony region and presence of sutures and may be influenced by the scalp. Characterising these responses may lead to improved physical surrogates and computational models for biomechanical simulations. The purpose of this study was to experimentally investigate the mechanical response of the human head to focal impacts across the frontal and parietal bones, and the coronal and sagittal sutures, with and without the scalp. A custom apparatus, comprising an instrumented electromagnetic linear actuator with a 10 mm diameter hemispherical impactor tip, was used to apply 1.66 m/s velocity impacts to 20 matched-pair (left-right) locations on six cadaveric specimens. Force-displacement response corridors, peak force, stiffness and displacement at peak force were extracted to describe the mechanical response. The force-displacement curves were distinct for impacts with and without the scalp. Both the presence/absence of scalp, and the cranial region, influenced the peak force, stiffness and displacement at peak force. Compared to impacts without the scalp, with the scalp present the peak force and stiffness decreased and the displacement at peak force increased. These findings provide insight into the scalp- and region-dependent response of the head during focal dynamic loading.

Keywords Cranial impact, compression, stiffness, peak force, impact response.

I. INTRODUCTION

Finite element (FE) models and physical surrogates are valuable tools for investigating the biomechanics of head and neck injuries and related injury protection strategies and devices. To ensure biofidelity, these models use experimental data obtained from human cadaver and animal studies to define material properties and validate model responses. While material properties are often derived from quasi-static tests, the impact scenarios that these models aim to simulate typically occur under dynamic loading conditions.

Previous experimental studies have focused on the mechanical response of the intact human head during impact [1-3], with (for example) a focus on fracture patterns [4-6] or brain deformation [2]. However, the role of the scalp on cranial response, and the potential difference in mechanical response of the cranial sutures versus regions with a typical diploe structure, have not received substantial attention. The scalp is the first tissue contacted during impact and has been associated with lowering the impact force and impact energy [7,8], while the cranial sutures have been shown to influence fracture patterns during impact [9]. Improved characterisation of the regional scalp-bone response may help improve computational models and physical surrogates of the head. The aim of this study was to experimentally investigate the mechanical response of the human head to focal moderate-velocity impacts across the frontal and parietal bones, and the coronal and sagittal sutures, with and without the scalp.

II. METHODS

Specimen preparation

Ethical approval was granted by the University of Adelaide ethics committee (H-2024-077). Six cadaveric heads (75±5 year-old (yo), 3 male; mandible removed) underwent computed tomography (CT) (Biograph64, Siemens, Germany; 0.4 x 0.4 x 0.6 mm voxels) to screen for fractures or abnormalities, and to identify landmarks to define the test grid. Specimens were stored at -20°C and thawed at room temperature

C. F. Jones (e-mail: claire.jones@adelaide.edu.au) is Associate Professor of Biomechanics and D. Thompson-Bagshaw is a PhD student at University of Adelaide in Australia. N. S. Reitsma is a MSc student and B. Sandoz is Associate Professor of Biomechanics at Arts et Métiers Institute of Technology in France. Z. Glover is a BASc student at Queens University in Canada.

(21°C) for at least two days prior to testing. Phosphate-buffered saline was applied throughout to maintain hydration. The crania were sectioned at the plane defined by the zygomaticofrontal sutures and the inion using an oscillating saw and the intracranial tissue was removed from the superior portion. Approximately 3 cm of bone was exposed around the base of each specimen and six screws were inserted, augmented with wire, and embedded with dental stone in a custom mould with a silicon plug. After curing, the mould was inverted and the plug removed; to simulate brain tissue [10,11], the crania were filled with gelatin (Gelita Ltd., Christchurch, New Zealand; 5 g/100 mL) and refrigerated overnight. Assuming cranial symmetry, the scalp and periosteum were removed from one side while the other side was maintained intact and was clean shaven. Using a specimen-specific CT-informed template, 20 left-right matched-pair impact locations were marked corresponding to the frontal (n=3) and parietal (n=3) bones, and coronal (n=2) and sagittal sutures (n=2).

Mechanical loading

Each test location underwent a single impact using a custom-built testing apparatus (Appendix Fig. A1), consisting of an electromagnetic linear actuator (LinMot, Switzerland) held vertically in a frame that was floor-mounted and clamped to a vertical support structure. The impactor was a stainless-steel cylinder (10 mm diameter) with a hemispherical tip, which interfaced with the actuator via a force transducer (KM30z, ME-Meßsysteme GmbH, Germany; 10 kN or 20 kN). An accelerometer (7264B-500, Endevco Corp., USA) was mounted on the actuator. Impactor position was measured with a magnetic linear encoder (LM15, Rotary and Linear Motion Sensors, Slovenia). The linear actuator was controlled via the LinMot-Talk 6.9 software using the command table. The motion sequence was initiated by slowly raising the impactor by 120 mm, pausing for 50 ms, then accelerating downward towards the specimen to a nominal velocity of 1.66 m/s. The motor was deactivated after 120 mm of downward travel (just prior to the specimen surface) allowing freefall and rebound thereafter. Load, acceleration, and position data were acquired at 50 kHz using a data acquisition system (cDAQ-9174, National Instruments, USA) and custom LabView software (National Instruments, USA). Two high-speed cameras (VEO 1010, Phantom, USA) recorded the frontal and side views of the impacts at 10 kHz. The specimen, in its embedding mould, was rigidly fixed to the specimen stage, which was then rotated about the y- and z-axes to align a hemispherical bubble level placed on the impact location in the horizontal plane, then translated along the y- and x-axes to align the impact location with the impactor tip axis. The impacts were performed in the following order: frontal (with and without scalp), parietal (with and without scalp), coronal suture (with and without scalp), and sagittal suture (with and without scalp). After each impact, the specimen was visually inspected for indication of bony damage. Following completion of the test sequence, post-test CT scans (NAEOTOM Alpha, Siemens, Germany; 0.2 x 0.2 x 0.2 mm voxel size) were obtained.

Data processing

Pre- and post-test CT images were used to measure skull thickness, bone mineral density and scalp thickness at each impact location, but these data are not reported herein. All impact data were processed using custom code (Matlab R2023b, MathWorks, USA). Force transducer and accelerometer data were filtered using a two-way, 2nd-order, low-pass Butterworth filter (cut-off frequency 2 kHz). Force data were inertially compensated using the impactor and ½ load cell mass and the measured acceleration. Encoder data were spline fit. Impact commencement was defined as 50 N, corresponding to time and displacement of zero. Impact completion was defined as the peak force. Force-displacement response corridors (mean and standard deviation) were derived using the ArcGen method [12] for each combination of scalp condition and impact region. To extract stiffness, defined as the slope of the force-displacement curve, two methods were employed depending on whether the scalp was present or not. For impacts with scalp, the Matlab toolbox SLMengine was used iteratively to first identify the transition from the low (k0) to high stiffness region, then to fit a bilinear approximation (k1, k2) across the high stiffness region. For data without scalp, the first iteration was redundant (i.e. no low stiffness region), so only the final bilinear approximation (k1, k2) was determined. The stiffness reported herein is k1.

Statistics

Three linear mixed-effect models were developed in SPSS (v29, IBM) to assess the effect of scalp presence (yes/no) and cranial region (frontal/parietal/coronal suture/sagittal suture) on (1) peak force, (2) stiffness, k1, and (3) displacement at peak force. These models included specimen ID as a random effect.

III. RESULTS

Across all specimens, 120 impacts were completed. No soft or bony tissue damage extended beyond the immediate impact sites, so repeated tests across the crania were considered acceptable. All frontal impacts for ID05 were excluded due to isolated abnormal bone growth across this region. Four impacts of ID01 were excluded due to deflection of the impactor during loading (visualised on high-speed video), which likely occurred due to oblique alignment of the skull surface relative to the actuator. At the impact location, bony damage consisted of local indentation of the outer cortical mantle; no fractures of the inner mantle were detected. Scalp damage included local plastic compression and rupture. High-speed video showed the measured displacement comprised a combination of local scalp and/or bone deformation, and deflection (flexure) of the surrounding bone.

Force-displacement curves for each impact, and corresponding response corridors generated for each region, showed differing responses for impacts on scalp-bone versus bone only (Fig. 1). Bone impacts were characterised by a relatively steeper (usually) single quasilinear region, whereas scalp-bone impacts had a substantial low stiffness region that transitioned to a steeper quasilinear region at around 2–4 mm displacement.

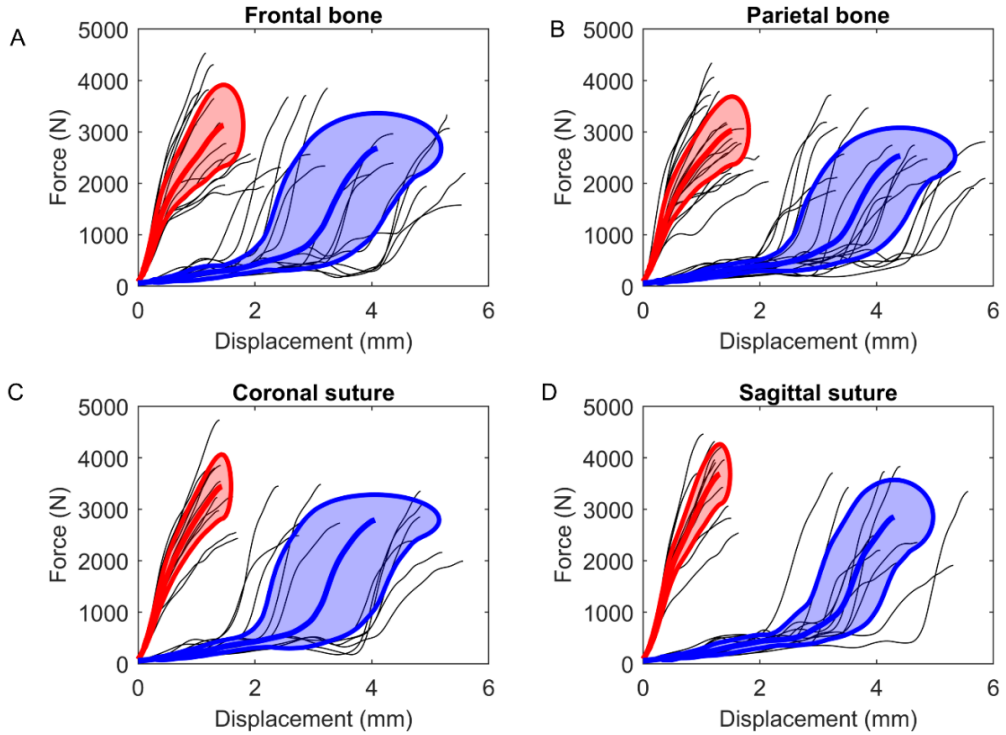

Fig. 1. Comparison of bone (red) and scalp-bone (blue) force-displacement response corridors for impacts to the (A) frontal bone, (B) parietal bone, (C) coronal suture, and (D) sagittal suture. Black lines correspond to force-displacement data for each impact test across all specimens.

Both the presence of scalp and the cranial region influenced the peak force, stiffness and displacement at peak force (Fig. 2; Appendix, Tables AI–AIII). Compared to impacts without the scalp, with the scalp present the peak force (Appendix, Table AI) and stiffness (Appendix, Table AII) decreased and the displacement at peak force increased (Appendix, Table AIII) (Fig. 2). Peak force generally increased from parietal, to frontal, then coronal suture and sagittal suture, with differences detected between parietal and both suture locations, and between frontal and the sagittal suture. Stiffness (k1) generally increased from parietal to frontal, and from coronal to sagittal suture; however, a difference was detected only between the parietal and sagittal suture regions. Displacement at peak force was greater for the sagittal compared to the coronal suture.

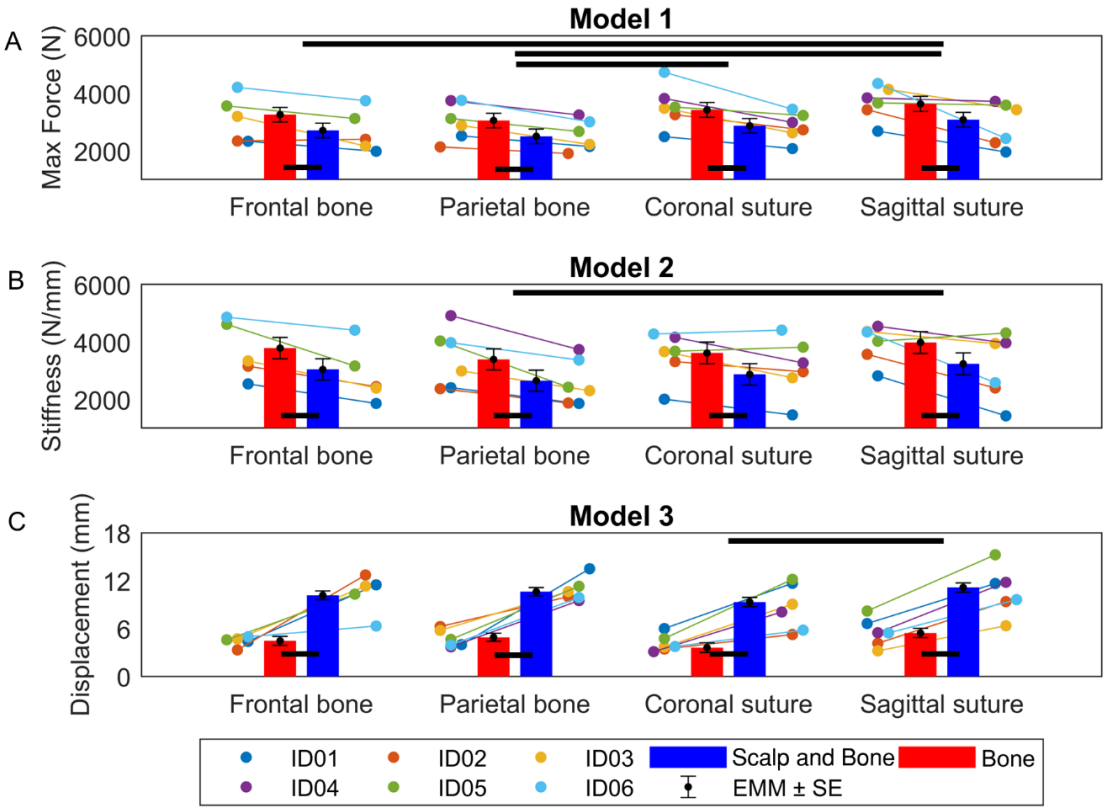

Fig. 2. Comparison of (A) peak force, (B) stiffness, and (C) displacement at peak force, by cranial region, for bone (red bars) and scalp-bone (blue bars) test locations. Paired data (coloured dots) are the mean of the impact test locations for each specimen ID in each region (frontal and parietal: n=3; coronal and sagittal suture: n=2). Vertical bars correspond to the estimated marginal mean (EMM), and black circle and whiskers correspond to the EMM ± SE, from each linear mixed model. Horizontal black bars represent statistically significant ($p \leq 0.05$) post-hoc pair-wise comparisons.

IV. DISCUSSION

Focal repeated impacts (1.66 m/s) were performed across four cranial regions, in a matched-pairs with/without scalp experimental design, on six cadaveric heads. The force-displacement curves were distinctly different for the two scalp conditions, with the presence of scalp producing an initial low stiffness region of substantial length. Linear mixed models identified an overall dependence of both scalp presence and cranial region on peak force, stiffness (k1) and displacement at peak force. Force-displacement response corridors, albeit specific to the test setup and specimen boundary conditions, were developed for each impact type.

The impacts resulted in focal indentation of the outer cranial mantle, and potentially some damage to the underlying cancellous bone, but no frank fractures or disruption of the inner cranial mantle were observed. This tissue damage outcome was paired with a bilinear response in the high-stiffness region for most impacts. Some studies have attributed the bilinear force-displacement response to sequential fracture of the outer and inner mantle [4,13], while others have similarly observed this response without cranial fracture [3].

The mean±SD peak force with scalp was 2711±642 N, and without scalp 3276±729 N, which is lower than values previously reported for whole heads: 4881±447 N at 1 m/s, 7772±2007 N at 2 m/s [3], 5938 N at 3.6 m/s [4], and 5000 N at 2.7 m/s [14]. Peak force is likely heavily influenced by test and specimen configuration. Removing the scalp increased the peak force by 20%, which is less than the 35% previously reported [7].

The mean stiffness (k1) in this study was 3617±1041 N/mm without scalp and 2854±997 N/mm with scalp. These values are higher than the 1799±881 N/mm stiffness reported for drop tower tests conducted on the temporo-parietal region of the head with scalp at 2.7 m/s [14], but similar to reported mean stiffness of 2487±558 N/mm for 1 m/s impacts and 2934±1898 N/mm for 2 m/s impacts to the vertex of whole heads with scalp [3]. This study observed higher stiffness for the sagittal suture compared to the parietal bone, which is dissimilar to the lower bending stiffness observed for sutures compared to the parietal bone in three-point bending on cranial

tokens [15].

This experimental study has some limitations. The number of specimens was relatively low, but the outcomes were made more robust with a matched-pairs within-specimen design. Specimens were defrosted from fresh frozen prior to use; freezing may have had some effect on scalp properties, but this was unavoidable. Despite the test apparatus being rigidly fixed to a support structure and robustly designed, there was some movement of the specimen stage during impact and this support stiffness may have varied across the various tilt angles used to position the specimen surfaces tangential to the impactor tip. However, high-speed video showed that this motion occurred after peak displacement and data were not analysed beyond this point. Further analysis is required to determine if regional-specific responses are related to scalp thickness, bone thickness and/or bone density at the impact locations.

V. CONCLUSION

This study provides valuable insights into the mechanical response of the human cranium to localised impacts, highlighting the significant influence of both cranial region and the presence of the scalp. The experimental results demonstrate that the scalp reduces peak force and stiffness while increasing displacement at peak force, compared to impacts on bone alone. These findings underscore the importance of considering scalp presence in biomechanical models and physical surrogates to enhance their biofidelity. The distinct force-displacement response corridors developed for different cranial regions and scalp conditions can serve as reference data for future computational, surrogate and experimental studies. Further research is warranted to explore the underlying mechanisms and to extend these findings to a broader range of impact conditions and cranial regions.

VI. ACKNOWLEDGEMENTS

The authors acknowledge the facilities and scientific and technical assistance of the National Imaging Facility, a National Collaborative Research Infrastructure (NCRIS) capability, at the Large Animal Research and Imaging Facility (LARIF) and Clinical Research Imaging Centre (CRIC), South Australian Health and Medical Research Institute (SAHMRI). The authors also acknowledge support from Professor Nigel Jones (FRACS) in medical image review. The study was funded, in part, by the Australian Research Council (DP190101209: CFJ).

VII. REFERENCES

[1] Loyd, A.M., Nightingale, R.W., et al. The response of the pediatric head to impacts onto a rigid surface. *J Biomech*, 2019. 93: p. 167-176

[2] Hardy, W.N., Mason, M.J., et al. A study of the response of the human cadaver head to impact. *Stapp Car Crash J*, 2007. 51: p. 17-80

[3] Thompson-Bagshaw, D.W., Quarrington, R.D., Dwyer, A.M., Jones, N.R., and Jones, C.F. The Structural Response of the Human Head to a Vertex Impact. *Ann Biomed Eng*, 2023. 51(12): p. 2897-2907

[4] Delye, H., Verschueren, P., et al. Biomechanics of frontal skull fracture. *J Neurotrauma*, 2007. 24(10): p. 1576-86

[5] Yoganandan, N., Zhang, J., and Pintar, F. Force and acceleration corridors from lateral head impact. *Traffic Inj Prev*, 2004. 5(4): p. 368-73

[6] Gurdjian, E.S., Webster, J.E., and Lissner, H.R. The mechanism of skull fracture. *Radiology*, 1950. 54(3): p. 313-39

[7] Gurdjian, E.S. Recent advances in the study of the mechanism of impact injury of the head--a summary. *Clin Neurosurg*, 1972. 19: p. 1-42

[8] Trotta, A., Zouzias, D., De Bruyne, G., and Ni Annaidh, A. The Importance of the Scalp in Head Impact Kinematics. *Ann Biomed Eng*, 2018. 46(6): p. 831-840

[9] Ptak, M., Ratajczak, M., et al. Investigation of biomechanics of skull structures damages caused by dynamic loads. *Acta Bioeng Biomech*, 2018. 20(4): p. 143-150

[10] Falland-Cheung, L.S., M; Hammer, N; Waddell, J.N.; Tong, D.C.; Brunton, P.A. Elastic behavior of brain simulants in comparison to porcine brain at different loading velocities. *Journal of the Mechanical Behavior of Biomedical Materials*, 2018. 77: p. 609-615

[11] Singh, D., Boakye-Yiadom, S., and Cronin, D.S. Comparison of porcine brain mechanical properties to potential tissue simulant materials in quasi-static and sinusoidal compression. *J Biomech*, 2019. 92: p. 84-91

[12] Hartlen, D.C. and Cronin, D.S. Arc-Length Re-Parametrization and Signal Registration to Determine a Characteristic Average and Statistical Response Corridors of Biomechanical Data. *Front Bioeng Biotechnol*, 2022. 10: p. 843148

[13] Yoganandan, N., Pintar, F.A., et al. Biomechanics of skull fracture. *J Neurotrauma*, 1995. 12(4): p. 659-68

[14] Allsop, D., Thomas R. Perl, and Warner., C.Y. Force/Deflection and Fracture Characteristics of the Temporo-Parietal Region of the Human Head. *SAE Transactions* 1991. 100: p. 2009–18.

[15] Delille, R.L., D.; Potier, P.; Drazetic, P.; Markiewicz, E. . Experimental study of the bone behaviour of the human skull bone for the development of a physical head model. *International Journal of Crashworthiness*, 2007. 12(2): p. 101–108

VIII. APPENDIX

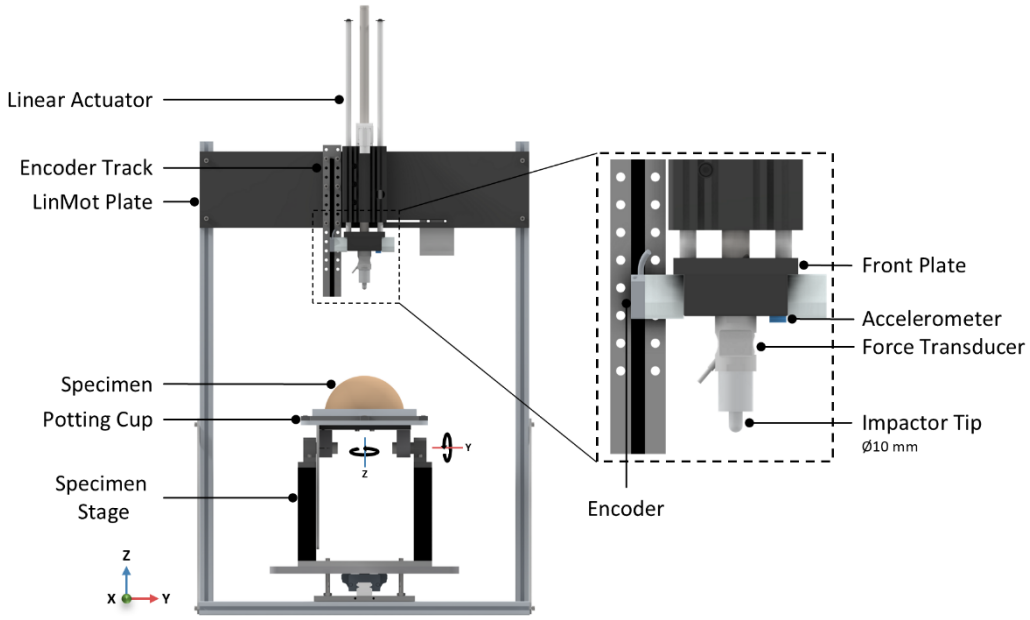

Fig. A1. Schematic of custom test apparatus. The specimen was positioned within the potting cup, fixed to the specimen stage, which enabled rotation about the y- and z-axes and translation along the x- and y-axes. Positioned above the specimen is the linear actuator, which moves the front plate along the z-axis.

TABLE AI

PEAK FORCE, LINEAR MIXED MODEL OUTPUT

Parameter	Estimate	95% Confidence Interval	p-value
Intercept	3082.5	[2456.4, 3708.7]	<0.001
SpecimenType=Bone	550.1	[407.7, 692.5]	<0.001
SpecimenType=SkinBone	-		
Region=Coronal suture	-211.8	[-442.2, 18.7]	0.071
Region=Frontal	-374.5	[-596.1, -152.9]	0.001
Region=Parietal	-578.4	[-791.1, -365.7]	<0.001
Region=Sagittal suture	-		

TABLE AII

STIFFNESS, LINEAR MIXED MODEL OUTPUT

Parameter	Estimate	95% Confidence Interval	p-value
Intercept	3233.8	[2332.1, 4135.6]	<0.001
SpecimenType=Bone	743.6	[493.6, 993.6]	<0.001
SpecimenType=SkinBone	-		
Region=Coronal suture	-367.1	[-771.6, 37.4]	0.075
Region=Frontal	-196.3	[-585.2, 192.6]	0.319
Region=Parietal	-589.7	[-963.0, -216.4]	0.002
Region=Sagittal suture	-		

TABLE AIII

DISPLACEMENT AT PEAK FORCE, LINEAR MIXED MODEL OUTPUT

Parameter	Estimate	95% Confidence Interval	p-value
Intercept	-11.2	[-12.4, -9.9]	<0.001
SpecimenType=Bone	5.7	[4.9, 6.5]	<0.001
SpecimenType=SkinBone	-		
Region=Coronal suture	1.8	[0.6, 3.1]	0.004
Region=Frontal	1.0	[-0.2, 2.1]	0.098
Region=Parietal	0.5	[-0.5, 1.6]	0.330
Region=Sagittal suture	-		